UC Berkeley
UC Berkeley Previously Published Works

Title
Nanoscale Electrochemical Phenomena of Polarization Switching in Ferroelectrics

Permalink
https://escholarship.org/uc/item/1z86c6kh

Journal
ACS Applied Materials & Interfaces, 10(44)

ISSN
1944-8244

Authors
Ievlev, Anton V
Brown, Chance C
Agar, Joshua C
et al.

Publication Date
2018-11-07

DOI
10.1021/acsami.8b13034

Peer reviewed

eScholarship.org Powered by the California Digital Library
University of California

Nanoscale Electrochemical Phenomena of Polarization Switching in Ferroelectrics

Anton V. Ievlev[1,2,*], Chance C. Brown[1,3], Joshua C. Agar[4], Gabriel A. Velarde[4], Lane W. Martin[4], Alex Belianinov[1,2], Petro Maksymovych[1,2], Sergei V. Kalinin[1,2] and Olga S. Ovchinnikova[1,2*]

[1]The Center for Nanophase Materials Sciences, Oak Ridge National Laboratory,
1 Bethel Valley Rd., Oak Ridge, TN 37831
[2]Institute for Functional Imaging of Materials, Oak Ridge National Laboratory,
1 Bethel Valley Rd., Oak Ridge, TN 37831

[3]The Bredesen Center, University of Tennessee, 821 Volunteer Blvd, Knoxville, TN 37920

[4]Department of Materials Science and Engineering, University of California Berkeley, Berkeley, California 94720, USA

*Authors to whom correspondence should be addressed. Email:

ievlevav@ornl.gov, ovchinnikovo@ornl.gov

Notice: This manuscript has been authored by UT-Battelle, LLC, under Contract No. DE-AC0500OR22725 with the U.S. Department of Energy. The United States Government retains and the publisher, by accepting the article for publication, acknowledges that the United States Government retains a non-exclusive, paid-up, irrevocable, world-wide license to publish or reproduce the published form of this manuscript, or allow others to do so, for the United States Government purposes. The Department of Energy will provide public access to these results of federally sponsored research in accordance with the DOE Public Access Plan (http://energy.gov/downloads/doe-public-access-plan).

Abstract

Polarization switching is a fundamental feature of ferroelectric materials, enabling a plethora of applications, and captivating the attention of the scientific community for over half a century. Many previous studies considered ferroelectric switching as a purely physical process; where polarization is fully controlled by the superposition of electric fields. However, screening charge is required for thermodynamic stability of the single domain state that is of interest in many technological applications. The screening process has always been assumed to be fast; thus the rate limiting phenomena were believed to be domain nucleation and domain wall dynamics. In this manuscript, we demonstrate that polarization switching under an atomic force microscopy tip leads to reversible ionic motion in the top three nanometers of $PbZr_{0.2}Ti_{0.8}O_3$ surface layer. This evidence points to a strong chemical component to a process believed to be purely physical, and has major implications for understanding ferroelectric materials, making ferroelectric devices, and interpreting local ferroelectric switching.

Keywords

Ferroelectrics, Screening, Chemical phenomena, Ionic motion, Atomic force microscopy, Time-of-flight secondary ion mass spectrometry

Introduction

Polarization switching in ferroelectric materials underpins a broad gamut of applications ranging from random access memory,[1] tunneling barriers,[2-4] data storage,[5] and ferroelectric ceramics.[6] Classically, the polarization switches due to a co-existence of energetically equivalent crystallographic states, that can be altered with an external electric field. To stabilize single domain state, charge discontinuity at surfaces and interfaces requires compensation, or screening, to avoid long-range electrostatic fields that destabilize the ferroelectric phase. Therefore, in materials and applications relying on polarization switching, a chemical change – the reconfiguration of screening charges, also needs to be taken into account.

In a simple picture of a metal-ferroelectric interface, the screening charge comes from metal's conduction band. The difference in the location of the screening charge, and polarization-bound charge leads to convoluted behavior, described by the effective dielectric dead layer approximation. Screening at surfaces and interfaces is more complex, and can be induced by either semiconductor-like band bending,[7-8] or adsorption of ionic species;[9-17] and can also be supported by the electrostatic energy reduction due to the domain structure reorganization. The effect of screening charge dynamics on polarization screening has been described, and was shown to produce unusual phenomena such as chaos, as well as fractal domain formation.[18-20] In all cases, the polarization screening is assumed to be chemically inert; leaving the composition of the ferroelectric intact.

However, analysis of extant ferroelectric phenomena suggests higher complexity. It is well known that multiple polarization switching cycles can accumulate damage at interfaces, dubbed "ferroelectric fatigue." Typically tens, or hundreds of thousands switching events are required, and the exact mechanisms remain controversial.[21-22] Furthermore, polarization-dependent photovoltaic effects in perovskites,[23-24] and built-in potentials in compositionally graded ferroelectric thin films[25] suggest that even under optimal screening conditions a considerable electric field remains in the material. Thus, switching is associated with high fields, which can chemically alter material composition.

In this work we utilize time of flight mass spectrometry secondary ion mass spectrometry (ToF-SIMS) combined with atomic force microscopy (AFM) to explore the structure property interplay of ferroelectric films during switching. Using this multimodal chemical imaging approach, we demonstrate that local ferroelectric switching by the AFM tip, significantly alters the chemical composition in the top 3 nm of the ferroelectric film. Specifically, we observe the formation of a double layer, or a concentration wave, of lead ions at the vicinity of the freshly polled region in a $PbZr_{0.2}Ti_{0.8}O_3$ thin film. This chemical phenomenon is reversible with bias of opposite polarity or spontaneous polarization direction. To model this behavior, we implemented numerical simulations of cations driven by an external electric filed in terms of a drift-diffusion model, which qualitatively demonstrated similar ion distribution near the surface of a polled ferroelectric film. This

work highlights the importance of chemical phenomena in understanding the physical process of the ferroic response.

Experiment and results

We used 100 nm thick ferroelectric lead zirconate titanate $PbZr_{0.2}Ti_{0.8}O_3$ (PZT) on 30 nm $SrRuO_3$ bottom electrode. Experiments have been carried out using TOF.SIMS NSC (ION-TOF, Germany), a combinatorial ToF-SIMS AFM in an ultra-high vacuum chamber with pressure 5×10^{-9} mbar or better. AFM tip has been used to locally switch polarization reversal by application of DC voltage of ±4V and piezoresponse force microscopy mode (PFM) has been further used to image resulted domain structure. In PFM mode AC voltage with amplitude 0.5 V and frequency 300 kHz were applied to the tip and signals of amplitude and phase of piezoresponse were measured. ToF-SIMS was used to study local chemical composition in thin surface layer of switched PZT. Measurements were run in positive ion detection mode with Bi_3^+ primary ion beam focused down to 120 nm. More details about experimental conditions can be found in Supplementary materials Section 1.

The experiments were performed in four steps: (1) The PZT surface was cleaned using an O_2^- sputter gun. Previous work has been shown, that sputtering with O_2^- is an effective way to clean and thin ferroelectric thin films, while preserving their ferroelectric properties.[26] (2) Cleaned areas were switched using a biased AFM tip, and subsequently imaged by piezoresponse force microscopy (PFM). (3) Chemical changes of the surface and the bulk of

the switched regions were analyzed by ToF-SIMS using a Bi_3^+ liquid metal ion gun and time-of-flight mass detector. (4) The depth of the sputtered crater after ToF-SIMS measurements was measured by contact mode AFM. The cleaning step was essential to reveal chemical changes associated with ferroelectric phenomena and not altered by surface contamination, which can affect chemistry of the sample due to the electric field application.[27]

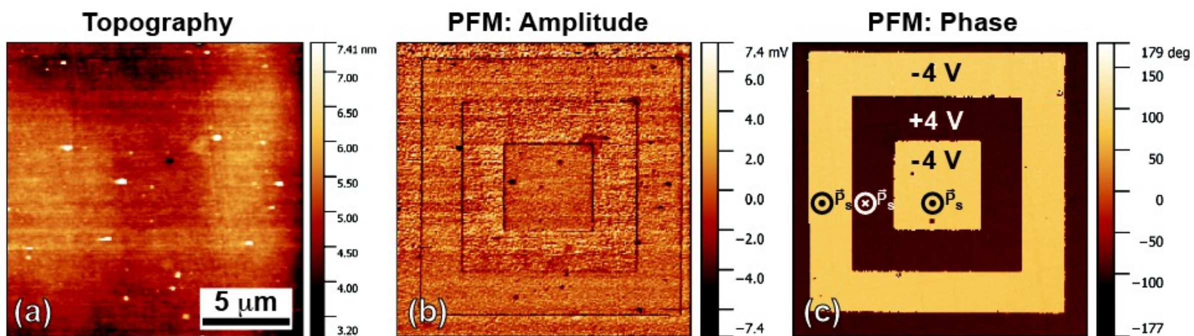

Figure 1. PFM measurements of the piezoresponse in the locally switched regions of a PZT thin film. (a) Topography, (b) PFM amplitude signal, (c) PFM phase signal.

Local polarization switching was induced by a conductive AFM tip with applied DC bias of ±4 V. PZT was switched by scanning a clean, square region (Fig. 1a) from 5 to 15 μm (details of the switching procedure can be found in Section 1 of *Supplemental Materials*) with a characteristic nested domain pattern shown in figure 1(b, c). The outermost 15 μm square and the innermost 5 μm square have a reversed spontaneous polarization (directed upwards), while the middle 10 μm area was switched back to the initial,

downward direction, of spontaneous polarization. All produced domain structures were found to be stable – no changes were observed for at least 24 hours.

ToF-SIMS studies were performed inside the polled region. The time to switch between AFM and ToF-SIMS hardware did not exceeded 10 min, the sample remained in the chamber with base pressure unaffected. In ToF-SIMS the switched area was scanned multiple times with focused Bi_3^+ ion gun. This allowed ~120 nm lateral and sub-nanometer depth resolution. The AFM analysis of the sputtered crater (*Supplemental materials,* Fig. S1) was used to calibrate the chemical data depth, and reconstruct local chemical changes in the PZT surface layer.

ToF-SIMS data is hyperspectral, where a mass spectrum is measured at each spatial pixel in *x*, *y* and *z* direction. Averaged mass spectra over the whole dataset clearly shows the base PZT elements Pb^+, Zr^+ and Ti^+, as well as their oxides PbO^+, ZrO^+ and TiO^+ (Fig. 2a). Distribution of the peaks area as a function of spatial location allowed us to characterize local chemical changes in the studied area (3D dataset of all identified peaks can be found in *Supplemental Materials* Fig. S2). To simplify the data analysis and to understand the underlying chemical changes associated with reversible polarization switching we will focus our analysis on the most pronounced peaks – Pb^+ and Ti^+ (Fig. 2b-i). We should also note, that in our research we used positive ion detect mode, which didn't allow to identification of negative oxygen ions.

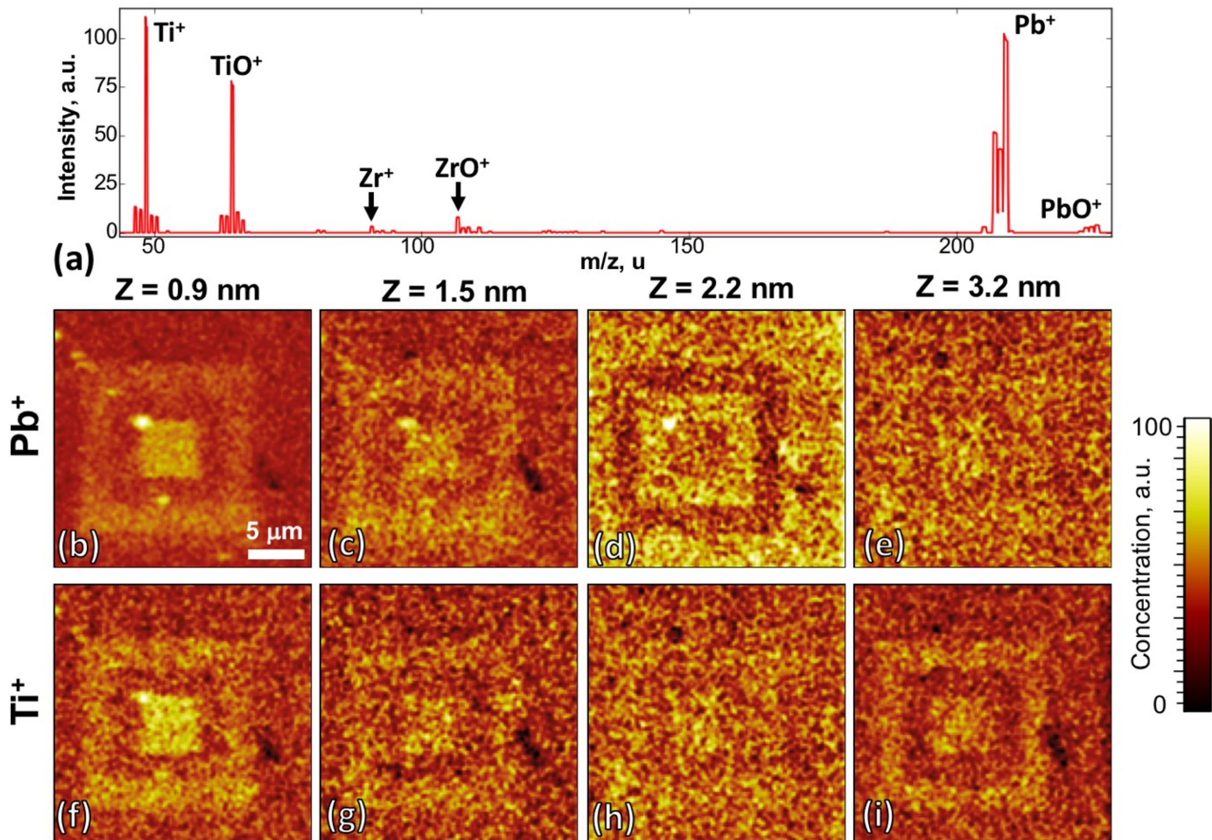

Figure 2. ToF-SIMS in the ferroelectrically switched region. (a) Averaged mass spectrum and (b-i) ToF-SIMS chemical maps of spatial distribution of base elements at different depths. (b-e) Pb^+ and (f-i) Ti^+ ions at (b, f) 0.9 nm; (c, g) 1.5 nm; (d, h) 2.2 nm and (e, i) 3.2 nm of the depth respectively.

All surface measurements revealed an increase in the concentration of base elements in the scanned regions (Supplemental Materials, Fig. S3) as well as a significant amount of Si^+ (Supplemental Materials, Fig. 4). The presence of Si^+ is due to the surface contamination by silicone oils, which originates from the poly-dimethyl siloxane (PDMS) gel boxes, used for tips storage.[28-29] This contamination affected only a thin top layer of material (~1

nm), which is excluded from data analysis. Si concentration was found to be independent of domain polarity, and hence is not expected to affect the domain-specific phenomena.

Furthermore, the concentration of Pb^+ and Ti^+ clearly correlate with spontaneous polarization direction (Fig. 2(b-i), Fig. 3) deeper in the film. Specifically, both elements are more concentrated near the surface with upward polarization direction, or polled by a negative bias Fig. 2(b, c, f, g). However, at a depth of ~ 2.2 nm Pb^+ contrast inverts, with concentration decreasing in the negatively poled regions (Fig. 2d), while Ti^+ distribution at the same depth is almost uniform. Notably, the back-switched region at the 10 μm square, with downward polarization, didn't reveal any chemical changes with respect to the pristine sample at all depths. PFM imaging after ToF-SIMS characterization revealed, that domain structure has been almost completely erased, which may be due to interaction with ion beams or removal of the top screening layer.

ToF-SIMS data, represented as a depth profile averaged over switched regions and normalized to the depth profile of the pristine sample, is shown in Fig. 3c. Two regions are presented: (1) outer 15 μm square region with polarization reversed (upwards) with respect to pristine sample shown by a red line and (2) middle 10 μm back-switched region shown by a blue line. Concentration of Ti^+ and Pb^+ inside the back-switched region was found to be identical to the pristine sample. In the switched region, the concentration for both elements increases near the surface. We report a 7% and 4% increase

in concentration for Pb^+ and Ti^+ respectively. At about 1.7 nm into the sample, the concentration of both elements decreases to the value of the pristine sample. The decreasing trend continues for Pb+, reaching its minimum of -2% at a depth of 2.2 nm. Simultaneously, Ti^+ showed a slight increase at a depth of about 3 nm. The analysis of the Pb^+ depth profiles revealed the formation of a double layer, or a concentration wave, with higher concentration in the top layers (15 $\mu C/cm^2$ or ~19% of pristine sample) and depletion on the bottom (-6.3μ C/cm^2 or ~8.5% of pristine sample).

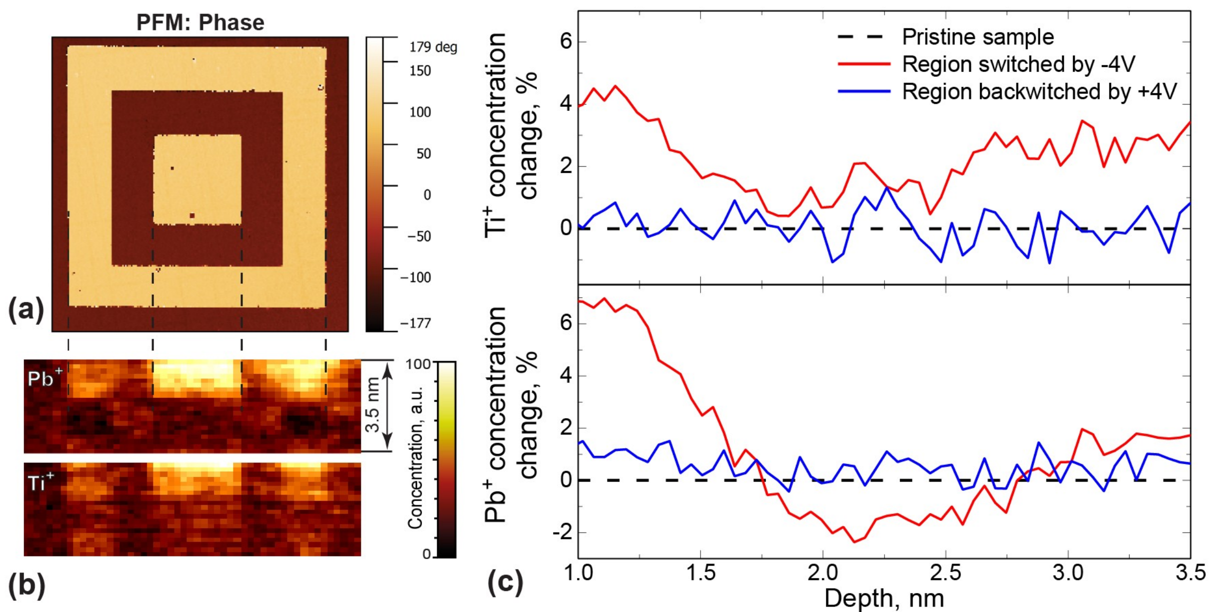

Figure 3. Local chemical changes in the bulk of PZT film, induced by local polarization switching. (a) PFM phase of polled regions; (b) corresponding ToF-SIMS X-Z map of Pb^+ and Ti^+; (c) depth profiles of local concentration changes with respect to the pristine sample of Ti^+(*top plot*) and Pb^+ (*bottom*

plot) within outer square switched by negative bias (*red line*) and middle square backswitched by positive bias (*blue line*).

To reveal global chemical changes in the sample across all possible elements, molecules, and functional groups, we used principal component analysis (PCA) on the multidimensional ToF-SIMS data.[30-32] In PCA mass spectrum X_i in each spatial point i is represented as a sum of averaged mass spectra e_0 and a linear combination of the orthogonal eigenvectors e_j with loading coefficients A_{ij}. The eigenvectors are sorted in descending order by variance. Thus, local changes in each point with respect to averaged mass spectrum can be characterized by a few first eigenvectors e_j and corresponding loading maps of the coefficients A_{ij}.

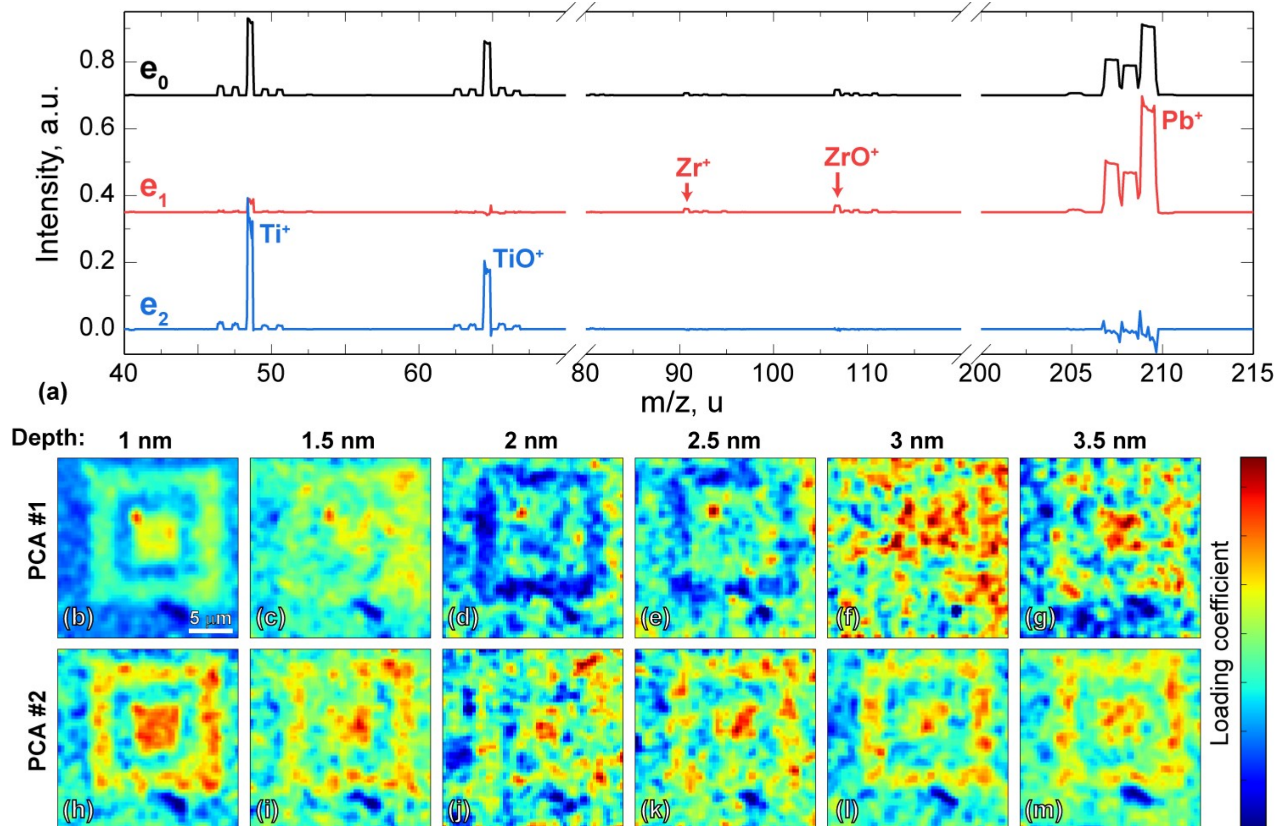

Figure 4. Results of the principal component analysis (PCA) on the ToF-SIMS data. (a) Averaged mass spectrum e_0 and first two eigenvectors. (b)-(m) Corresponding maps of loading coefficients at different depths (as labeled).

PCA of the chemical data collected from the switched PZT region, showed that the whole dataset can be characterized by only two eigenvectors (Fig. 4a), as the third eigenvector (*Supplemental Materials*, Fig. S5a) showed only changes in the peak shape (Fig. S5b). Analysis of the eigenvectors revealed, that the first eigenvector e_1, is the change in Zr^+, ZrO^+ and Pb^+ peaks with their isotopes, while the second eigenvector e_2 contains only peaks of Ti^+ and TiO^+. PCA loading maps (Fig. 4b), demonstrate the same trends as concentrations of Pb^+ and Ti^+ respectively, which allows

us to make a conclusion that Zr^+ and ZrO^+ concentrations demonstrate similar behavior to Pb^+. Similarly, TiO^+ shows same trend as Ti^+.

Summarizing, local ferroelectric switching by a biased AFM tip induces ion migration in the top 3 nm layer of PZT. Changes can be only found inside the regions where the polarization was switched with respect to pristine sample. These changes lead to formation of a Pb^+ concentration wave, with an induced charge of about 8-19% of the pristine sample. At the same time the backswitched region doesn't show any changes with respect to the pristine sample, which demonstrates reversibility of the induced chemical phenomena. Such results are in a good agreement with conception of dead layer, reducing depolarization field on the film interfaces.[33-34]

These chemical changes are likely to be caused by depolarization field, which in turn is caused by the unscreened charges on the freshly polled polar faces of the ferroelectric film. Commonly, screening is provided by charge redistribution in external electrodes, however with AFM tip induced switching, there is no top electrode. In this case observed phenomena is likely caused by the redistribution of the point defects in the vicinity of PZT surface. It's known that most common defects in PZT are represented by the oxygen and lead vacancies,[35] with oxygen vacancies having much higher values of mobility.[36] High values of the depolarization electric field in the surface vicinity leads to defects redistribution with creation of the screening layer, reducing total electric field. Low mobility of the lead ions in this case limits redistribution depth.

This process can be simulated in terms of a drift-diffusion model. In the simple 1D case cation concentration c along the axis z will be defined by Equation 1:

$$\frac{\partial c}{\partial t} = D \frac{\partial^2 c}{\partial z^2} + \frac{\partial}{\partial z}(cv) \tag{1}$$

where D is the diffusion coefficient, and v is the drift speed. Drift speed v can be directly proportional to the electric field produced by the biased AFM tip. Here we consider a spherical tip apex to calculate the drift speed, given by Equation 2:

$$v_x(z,t) = \mu_{ion} E_{tip}(z,t) = \mu_{ion} \frac{U_{tip}(t) R_{tip}}{(z + R_{tip})^2} \tag{2}$$

where μ_{ion} is the effective ion mobility, R_{tip} is the tip radius of curvature, and U_{tip} is the bias applied to the tip. Ion mobility, in turn, can be related with diffusion coefficient using Einstein relation in Equation 3:

$$D = \frac{\mu_{ion} k_B T}{q} \tag{3}$$

where k_B is the Boltzmann's constant, T is the temperature, and q is the ion charge. Using Equations (1) – (3) we performed numerical simulations of the ionic motion induced by the electric field of a biased AFM tip (Figure 5).

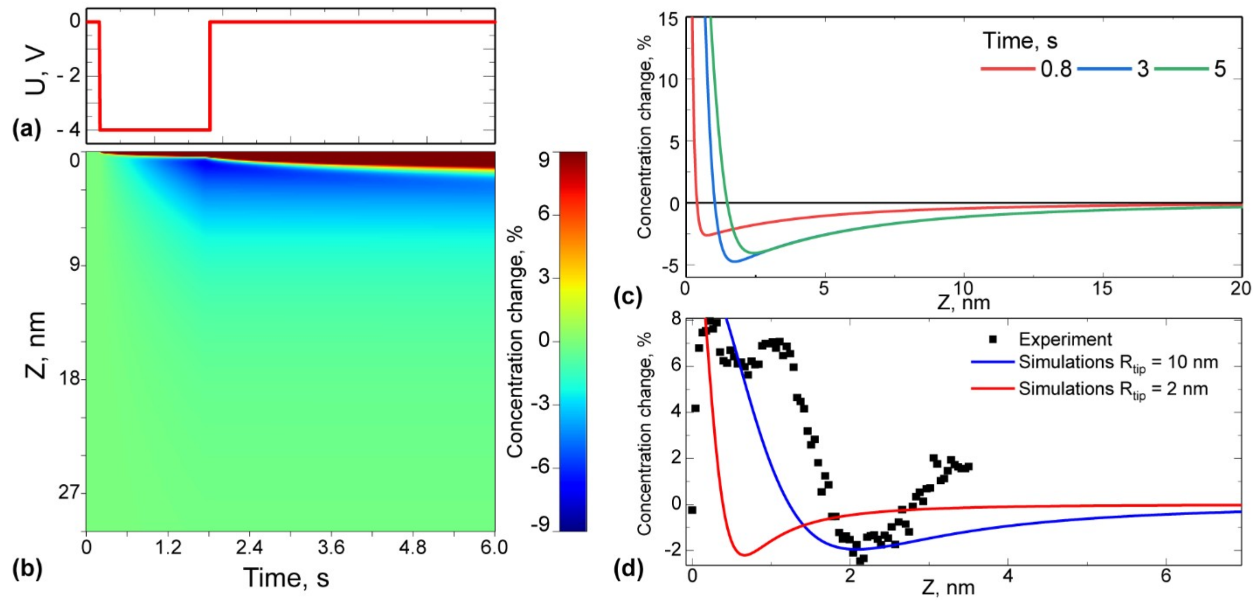

Figure 5. Drift-diffusion simulations of the ionic motion induced by electric field of biased AFM tip. (a) Pulse of the applied bias, used in simulations; (b) map of local cation concentration change induced by an AFM tip bias in coordinates of time and depth; (c), (d) depth profiles of the local change in concentration as a function of the time (c) and tip radius (d).

Initially concentration was uniformly distributed over the model $c(z,t)|_{t=0}=c_0$ and the boundary conditions excluded ionic flux through the edges. Electrical bias was simulated by a pulse with amplitude of 4 V and duration of 1.8 s (Fig. 5a). Calculations were performed in COMSOL Multiphysics finite element environment, and allowed us to observe local concentration change near the sample surface during application of the electric field and its relaxation after switching the field off (Fig. 5b).

As expected, simulations demonstrated the formation of a concentration wave near the surface (Fig. 5c), however the shape of the profile differed from experimentally observed data (Fig. 5d). We used a tip radius of about 10 nm, similar to what was used in the experiment. Concentration changed down to about 5 nm into the bulk, larger than the experimentally observed 2 nm. Simulations with a smaller tip radius showed wave localization near the sample surface, which also disagrees with experiment. These disagreement show that the used simple model cannot completely describe this system, since electrostatics, chemistry, screening, and depolarization are not considered. More precise model should consider electromigration as a self-consistent problem, where ionic motion change distribution of the electric fields and *vice versa*. In this case simulation should include Poison equation and mobility of the charge carriers. Such advanced simulation is beyond scope of the current work and will be published elsewhere. However, simple drift-diffusional model allowed to qualitatively show behavior similar to experiment, and adequately represents the formation of a concentration wave in the switched PZT. Values for the diffusion coefficient corresponding to best agreement with experiment were found to be around $D = 3.2 \times 10^{-19}$ m^2/s and corresponding lead ion mobility $\mu_{Pb} = 2.5 \times 10^{-16}$ $m^2/(V \cdot s)$.

Conclusion

In conclusion, we utilized a multimodal chemical imaging platform that combines atomic force microscopy with time-of-flight secondary ion mass spectrometry in ultra-high vacuum, to study the chemistry of local ferroelectric switching. Our data showed significant changes in the local concentration of the base elements in the top 3 nm thick surface layer of a lead zirconate-titanate thin film, after switching by an AFM tip. Lead ions formed a double layer, or a concentration wave within 2 nm from the sample surface. These chemical changes were found to be reversible and correlated with the direction of the spontaneous polarization. A drift-diffusion model was utilized to qualitatively explain the chemical changes. The simulation supplemented experiment and allowed us to attribute the observed phenomenon to cation motion induced by the superposition of electric fields near the surface of freshly switched ferroelectric film. We believe this insight will enhance the fundamental understanding of ferroelectric phenomena and aid in the practical application of ferroelectric materials in devices. For instance, explored chemical phenomena can be used to explain ferroelectric fatigue.

Supporting information

Supporting information supplies experimental details on AFM and ToF-SIMS experiments, as well as additional images on ToF-SIMS imaging, data analysis and depth calibration.

Acknowledgements

This research was conducted at the Center for Nanophase Materials Sciences, which is a DOE Office of Science User Facility, and using instrumentation within ORNL's Materials Characterization Core provided by UT-Battelle, LLC under Contract No. DE-AC05-00OR22725 with the U.S. Department of Energy.

References

1. Scott, J. F.; Dearaujo, C. A. P., FERROELECTRIC MEMORIES. *Science* **1989,** *246* (4936), 1400-1405.
2. Gruverman, A.; Wu, D.; Lu, H.; Wang, Y.; Jang, H. W.; Folkman, C. M.; Zhuravlev, M. Y.; Felker, D.; Rzchowski, M.; Eom, C. B.; Tsymbal, E. Y., Tunneling Electroresistance Effect in Ferroelectric Tunnel Junctions at the Nanoscale. *Nano Lett.* **2009,** *9* (10), 3539-3543.
3. Tsymbal, E. Y.; Kohlstedt, H., Applied physics - Tunneling across a ferroelectric. *Science* **2006,** *313* (5784), 181-183.
4. Maksymovych, P.; Jesse, S.; Yu, P.; Ramesh, R.; Baddorf, A. P.; Kalinin, S. V., Polarization Control of Electron Tunneling into Ferroelectric Surfaces. *Science* **2009,** *324* (5933), 1421-1425.
5. Ahn, C. H.; Tybell, T.; Antognazza, L.; Char, K.; Hammond, R. H.; Beasley, M. R.; Fischer, O.; Triscone, J. M., Local, nonvolatile electronic writing of epitaxial Pb(Zr0.52Ti0.48)O-3/SrRuO3 heterostructures. *Science* **1997,** *276* (5315), 1100-1103.
6. Setter, N.; Damjanovic, D.; Eng, L.; Fox, G.; Gevorgian, S.; Hong, S.; Kingon, A.; Kohlstedt, H.; Park, N. Y.; Stephenson, G. B.; Stolitchnov, I.; Tagantsev, A. K.; Taylor, D. V.; Yamada, T.; Streiffer, S., Ferroelectric thin films: Review of materials, properties, and applications. *Journal of Applied Physics* **2006,** *100* (5).
7. Fridkin, V. M., *Ferroelectric Semiconductors*. Springer: New York, 1980.
8. Vul, B. M.; Guro, G. M.; Ivanchik, II, ENCOUNTERING DOMAINS IN FERROELECTRICS. *Ferroelectrics* **1973,** *6* (1-2), 29-31.
9. Highland, M. J.; Fister, T. T.; Fong, D. D.; Fuoss, P. H.; Thompson, C.; Eastman, J. A.; Streiffer, S. K.; Stephenson, G. B., Equilibrium Polarization of Ultrathin PbTiO3 with Surface Compensation Controlled by Oxygen Partial Pressure. *Physical Review Letters* **2011,** *107* (18), 187602.
10. Highland, M. J.; Fister, T. T.; Richard, M. I.; Fong, D. D.; Fuoss, P. H.; Thompson, C.; Eastman, J. A.; Streiffer, S. K.; Stephenson, G. B., Polarization Switching without Domain Formation at the Intrinsic Coercive Field in Ultrathin Ferroelectric PbTiO3. *Physical Review Letters* **2010,** *105* (16), 167601.
11. Wang, R. V.; Fong, D. D.; Jiang, F.; Highland, M. J.; Fuoss, P. H.; Thompson, C.; Kolpak, A. M.; Eastman, J. A.; Streiffer, S. K.; Rappe, A. M.; Stephenson, G. B., Reversible Chemical Switching of a Ferroelectric Film. *Physical Review Letters* **2009,** *102* (4), 047601.
12. Fong, D. D.; Kolpak, A. M.; Eastman, J. A.; Streiffer, S. K.; Fuoss, P. H.; Stephenson, G. B.; Thompson, C.; Kim, D. M.; Choi, K. J.; Eom, C. B.; Grinberg, I.; Rappe, A. M., Stabilization of monodomain polarization in ultrathin PbTiO3 films. *Physical Review Letters* **2006,** *96* (12), 127601.
13. Kalinin, S. V.; Johnson, C. Y.; Bonnell, D. A., Domain polarity and temperature induced potential inversion on the BaTiO3(100) surface. *Journal of Applied Physics* **2002,** *91* (6), 3816-3823.

14. Kalinin, S. V.; Bonnell, D. A., Effect of phase transition on the surface potential of the BaTiO3 (100) surface by variable temperature scanning surface potential microscopy. *Journal of Applied Physics* **2000,** *87* (8), 3950-3957.
15. Kalinin, S. V.; Bonnell, D. A., Local potential and polarization screening on ferroelectric surfaces. *Physical Review B* **2001,** *63* (12), 125411.
16. Shur, V. Y.; Ievlev, A. V.; Nikolaeva, E. V.; Shishkin, E. I.; Neradovskiy, M. M., Influence of adsorbed surface layer on domain growth in the field produced by conductive tip of scanning probe microscope in lithium niobate. *Journal of Applied Physics* **2011,** *110* (5), 052017.
17. Ievlev, A. V.; Morozovska, A. N.; Shur, V. Y.; Kalinin, S. V., Humidity effects on tip-induced polarization switching in lithium niobate. *Applied Physics Letters* **2014,** *104* (9), 092908.
18. Ievlev, A. V.; Alikin, D. O.; Morozovska, A. N.; Varenyk, O. V.; Eliseev, E. A.; Kholkin, A. L.; Shur, V. Y.; Kalinin, S. V., Symmetry Breaking and Electrical Frustration during Tip-Induced Polarization Switching in the Nonpolar Cut of Lithium Niobate Single Crystals. *ACS Nano* **2015,** *9* (1), 769-777.
19. Ievlev, A. V.; Jesse, S.; Morozovska, A. N.; Strelcov, E.; Eliseev, E. A.; Pershin, Y. V.; Kumar, A.; Shur, V. Y.; Kalinin, S. V., Intermittency, quasiperiodicity and chaos in probe-induced ferroelectric domain switching. *Nature Physics* **2014,** *10* (1), 59-66.
20. Ievlev, A. V.; Morozovska, A. N.; Eliseev, E. A.; Shur, V. Y.; Kalinin, S. V., Ionic field effect and memristive phenomena in single-point ferroelectric domain switching. *Nature Communication* **2014,** *5*, 5545.
21. Scott, J. F.; Dawber, M., Oxygen-vacancy ordering as a fatigue mechanism in perovskite ferroelectrics. *Appl. Phys. Lett.* **2000,** *76* (25), 3801-3803.
22. Tagantsev, A. K.; Stolichnov, I.; Colla, E. L.; Setter, N., Polarization fatigue in ferroelectric films: Basic experimental findings, phenomenological scenarios, and microscopic features. *Journal of Applied Physics* **2001,** *90* (3), 1387-1402.
23. Kalinin, S. V.; Gruverman, A.; Bonnell, D. A., Quantitative analysis of nanoscale switching in SrBi[sub 2]Ta[sub 2]O[sub 9] thin films by piezoresponse force microscopy. *Appl. Phys. Lett.* **2004,** *85* (5), 795.
24. Haussmann, A.; Milde, P.; Erler, C.; Eng, L. M., Ferroelectric Lithography: Bottom-up Assembly and Electrical Performance of a Single Metallic Nanowire. *Nano Lett.* **2009,** *9* (2), 763-768.
25. Agar, J. C.; Damodaran, A. R.; Velarde, G. A.; Pandya, S.; Mangalam, R. V. K.; Martin, L. W., Complex Evolution of Built-in Potential in Compositionally-Graded PbZr1-xTixO3 Thin Films. *Acs Nano* **2015,** *9* (7), 7332-7342.
26. Ievlev, A. V.; Chyasnavichyus, M.; Leonard, D.; Agar, J. C.; Velarde, G. A.; Martin, L. W.; Kalinin, S. V.; Maksymovych, P.; Ovchinnikova, O. S., Subtractive fabrication of ferroelectric thin films with precisely controlled thickness. *Nanotechnology* **2018,** *29*, 155302.

27. Ievlev, A. V.; Maksymovych, P.; Trassin, M.; Seidel, J.; Ramesh, R.; Kalinin, S. V.; Ovchinnikova, O. S., Chemical State Evolution in Ferroelectric Films during Tip-Induced Polarization and Electroresistive Switching. *ACS Appl. Matt. Interf.* **2016,** *8* (43), 29588-29593.
28. Lo, Y. S.; Huefner, N. D.; Chan, W. S.; Dryden, P.; Hagenhoff, B.; Beebe, T. P., Organic and inorganic contamination on commercial AFM cantilevers. *Langmuir* **1999,** *15* (19), 6522-6526.
29. Ievlev, A. V.; Brown, C.; Burch, M. J.; Agar, J. C.; Velarde, G. A.; Martin, L. W.; Maksymovych, P.; Kalinin, S. V.; Ovchinnikova, O. S., Chemical Phenomena of Atomic Force Microscopy Scanning. *Anal. Chem.* **2018,** *90* (5), 3475-3481.
30. Jesse, S.; Kalinin, S. V., Principal component and spatial correlation analysis of spectroscopic-imaging data in scanning probe microscopy. *Nanotechnology* **2009,** *20* (8), 085714.
31. Biesinger, M. C.; Paepegaey, P. Y.; McIntyre, N. S.; Harbottle, R. R.; Petersent, N. O., Principal component analysis of TOF-SIMS images of organic monolayers. *Anal. Chem.* **2002,** *74* (22), 5711-5716.
32. Ievlev, A. V.; Belianinov, A.; Jesse, S.; Allison, D. P.; Doktycz, M. J.; Retterer, S. T.; Kalinin, S. V.; Ovchinnikova, O. S., Automated Interpretation and Extraction of Topographic Information from Time of Flight Secondary Ion Mass Spectrometry Data. *Sci. Rep.* **2017,** *7*.
33. Bratkovsky, A. M.; Levanyuk, A. P., Abrupt Appearance of the Domain Pattern and Fatigue of Thin Ferroelectric Films. *Physical Review Letters* **2000,** *84* (14), 3177-3180.
34. Bratkovsky, A. M.; Levanyuk, A. P., Continuous Theory of Ferroelectric States in Ultrathin Films with Real Electrodes. *Journal of Computational and Theoretical Nanoscience* **2009,** *6* (3), 465-489.
35. Boukamp, B. A.; Pham, M. T. N.; Blank, D. H. A.; Bouwmeester, H. J. M., Ionic and electronic conductivity in lead-zirconate-titanate (PZT). *Solid State Ionics* **2004,** *170* (3-4), 239-254.
36. Raymond, M. V.; Smyth, D. M., Defects and charge transport in perovskite ferroelectrics. *J. Phys. Chem. Solids* **1996,** *57* (10), 1507-1511.

Table of Content Graphic